Electrical Regeneration for Long-Haul Fiber-Optic Time and Frequency Distribution Systems

Przemysław Krehlik, Łukasz Śliwczyński, *Member, IEEE*, and Łukasz Buczek

***Abstract*— In recent years fiber-optic-based long-haul installations for time and frequency (T&F) distribution have become operational at various sites. The common practice to cope with large attenuation of long fiber path is to use bidirectional optical amplifiers. This, however, becomes insufficient in case of very long links and/or long spans between amplifiers, because of unavoidable deterioration of the signal-to-noise ratio (SNR). In this article, we present a solution where the optical signal amplification is combined with optical–electrical–optical (OEO) regeneration, performed in a few points along the link. We analyze the impact of replacing some optical amplifiers with OEOs and demonstrate the resulting improvement in terms of SNR of the received optical signal and the phase noise at the output of the T&F distribution system. Laboratory experiments performed with both spooled and metropolitan-area fibers (total length up to 900 km) confirmed the theoretical predictions and showed that placing the OEO regenerators in appropriate points along the link allows reaching the required SNR.**

***Index Terms*— Fiber optics, optical–electrical–optical (OEO) regeneration, time and frequency (T&F) transfer.**

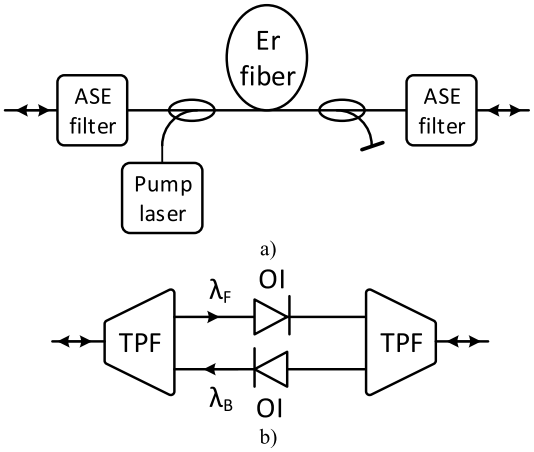

Fig. 1. Simplified scheme of (a) bidirectional amplifier and (b) WSI which may be cascaded with the amplifier. ASE stands for amplified spontaneous emission, TPF for three-port optical filter, and OI for optical isolator. λ_F and λ_B are the wavelengths of the forward and backward signals, respectively.

I. Introduction

THE very basic idea exploited in the most accurate and stable time and frequency (T&F) distribution is to use a single optical fiber for bidirectional exchange of signals. This way, thanks to the forward–backward symmetry of the propagation conditions, the impact of the environmental factors on signals' phase (and delay) may be reduced by orders of magnitude [1]–[8] when compared with unidirectional signaling. In addition, the same physical optical path for the forward and backward signals makes possible the absolute calibration of the time transfer [5], [9]. In case of long-haul links, when the attenuation of the optical path exceeds the power budget of the T&F distribution terminals, some means for bidirectional signals amplification are necessary. The most straightforward and elegant solution seems to be single-path bidirectional amplifiers (SPBAs), usually based on erbium-doped fiber [see Fig. 1(a)]. In this solution, the optical path for the forward and backward signals is exactly the same, and thus insertion of amplifiers does not affect the symmetry of the propagation conditions [10], [11].

Unfortunately, the bidirectional optical amplifiers are vulnerable to backscattered and reflected signals, which "circulate" around the amplifiers (see Fig. 2). The overlapping of the directly propagated signal with its fractions which undergoes double (or any even) backscattering and/or reflection generates a beating noise in the receiver, which can severely degrade the signal-to-noise ratio (SNR) at the receiver output, making it lower than the acceptable level [11]. Moreover, when the amplifier's gain is close to the round-trip losses of these "circulating" signals, the operation of the amplifier becomes unstable, or it can even start lasing, which leads to the total malfunction of the entire system. Because of that the maximum gain of bidirectional amplifiers is in practice limited to 15–20 dB. Yet another problem with bidirectional amplifiers is that their deployment decreases the power threshold for stimulated Brillouin scattering (SBS), which is the next factor

Manuscript received June 30, 2020; accepted August 6, 2020. Date of publication August 13, 2020; date of current version February 24, 2021. This work was supported in part by the TiFOON 18SIB06 Project through the EMPIR Program co-financed by the Participating States and the European Union's Horizon 2020 Research and Innovation Program and in part by the Faculty of Computer Science, Electronics and Telecommunications, AGH University of Science and Technology. *(Corresponding author: Przemysław Krehlik.)*

The authors are with the Faculty of Computer Science, Electronics and Telecommunications, AGH University of Science and Technology, 30-059 Kraków, Poland (e-mail: krehlik@agh.edu.pl).

Digital Object Identifier 10.1109/TUFFC.2020.3016610

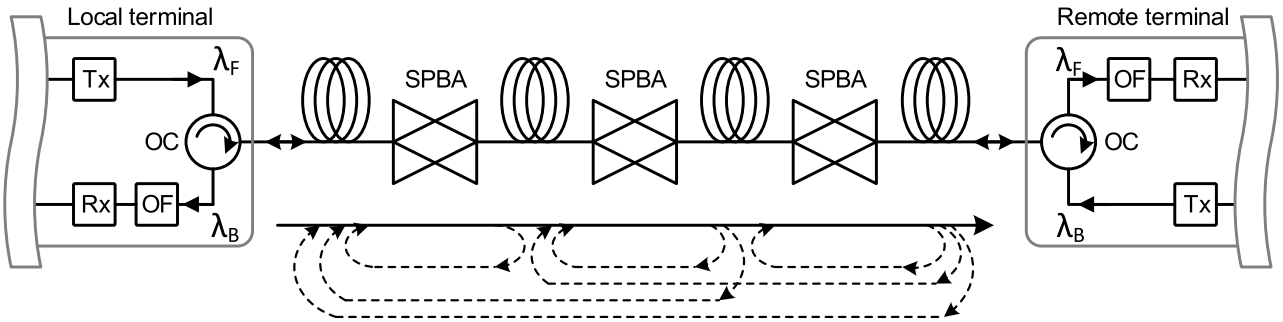

Fig. 2. Long-haul link with bidirectional amplifiers. At the bottom, the desired forward signal (solid-line arrow) and interfering signals resulting from double backscattering and reflections (dashed lines) are sketched. Note that single (an odd-order, in general) backscattering or reflections are not an issue as they may be eliminated by optical filters (OFs), provided slightly different wavelengths of local and remote Tx. OC stands for optical circulator and Rx for opto-electronic receiver.

limiting possible gain. Thus, finally the total gain of all the amplifiers must be substantially lower than the attenuation of the fiber [11], [12]. Operating a long-haul link with low-gain amplifiers also emphasizes the impact of their noises (in case of erbium-doped amplifiers generated mainly by amplified spontaneous emission—ASE), which negatively affects the SNR.

The partial solution to the problems mentioned above is to add wavelength selective isolators (WSIs) to the bidirectional amplifiers [see Fig. 1(b)]. Based on the fact as the forward and backward signals are carried on slightly different wavelengths λ_F and λ_B (usually distant by 100-GHz frequency offset), one may separate the signals with three-port optical filters (TPFs) and apply optical isolators for both the directions. The advantage is that this way the "circulation" of backscattered/reflected signals is eliminated, and higher gains of amplifiers may be set. Similar solutions were presented in [13] and [14], where the isolation for the backscattered signal is obtained in different topology. The common drawback of all these solutions is that the amplifier is no longer fully symmetrical. Careful assembly of the amplifier usually allows keeping the optical length difference for the forward and backward signals below 10 ps, but these offsets must be characterized and taken into account in the calibration of time distribution, which is quite a cumbersome procedure.

The other factor limiting the long-haul T&F distribution with fully optical amplification is a conversion of laser's optical phase noise to intensity noise (PN-IN), due to the optical signal interaction with the chromatic dispersion of the fiber [15]–[17]. This phenomenon is not related to any effects occurring in the optical amplifiers, but accumulates along the length of the (long) optical path.

To illustrate the above discussion with some numerical values, we simulated the bidirectional link with N sections of a fiber and $N-1$ amplifiers in a chain, as depicted in Fig. 2. We used the dedicated simulation tools developed for bidirectional links with SPBAs based on erbium-doped fiber [12]. The simulations took into account the beating noises resulting from amplifiers' ASE, the odd-order and even-order backscattering, the PN-IN conversion, and the shot and thermal noise of the receiver. In the simulations, we applied a typical value of the dispersion coefficient characteristic for G.652 fiber and the laser linewidth of 15 MHz (a value

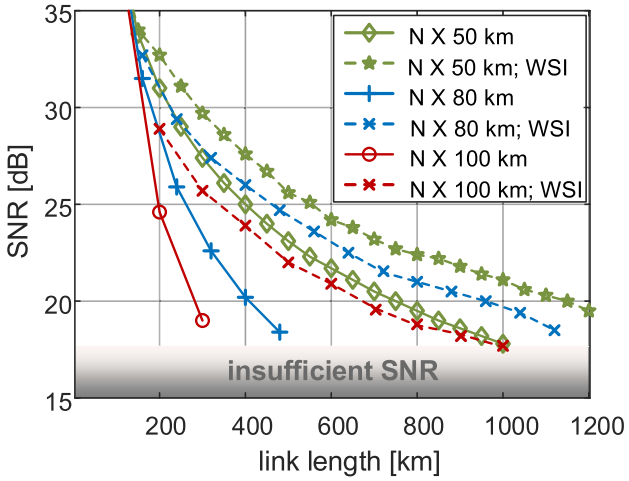

Fig. 3. Simulated SNR for different distances between the optical amplifiers, for both basic bidirectional amplifiers and the ones equipped with WSIs.

typical for telecom-grade DFB laser). The lengths of all the fiber sections were assumed equal, being either 50 or 80 km, or 100 km. We simulated both the cases with basic bidirectional amplifiers, and the one with all the amplifiers equipped with the WSIs. Fig. 3 presents the SNR calculated in the electrical domain at the output of the receiver, plotted versus the link length.

To discuss the results of the simulations, one should refer the obtained SNR to the values needed for proper operation of the T&F distribution system. Our experience in this matter is related to the ESTAB technology, where the phase (and delay) of the distributed T&F signals is actively stabilized by a pair of matched electronic delay lines, and on/off intensity modulation of optical signals is used [5]. In this particular solution, the lowering of the SNR begins to be noticeable after dropping below 25 dB, when the only observable result is a gradual increase in the jitter of the remote T&F signals. This effect is not very pronounced; for the SNR $= 20$ dB, the jitter rises from about 3 ps to some 6 ps. But for slightly lower SNR, sporadic phase jumps of the frequency signal and incidental loss of 1 PPS time pulses become observable. Thus, the SNR value of 17–18 dB should be regarded as the threshold for proper system operation. (In fact, this value is quite similar to the SNR required in telecom data transmission systems

TABLE I
EXAMPLES OF OPTICALLY AMPLIFIED LINKS

No.	Total length [km]	Total att. [dB]	Min/max span length [km]	No. of SPBAs	No. of WSIs	Simulated SNR [dB]	Operational status
1	421	117	5/65	8	2	25	since 2011
2	338	84	23/63	7	0	25	since 2015
3	223	51	46/76	3	0	27	since 2016
4	139	32	62/77	1	0	28	since 2016
5	388	98	61/91	4	4	24	since 2018
6	294	69	41/74	4	2	32	since 2018
7	774	235	34/96	11	0 - 11	6–19 (0–11 WSIs)	insufficient SNR

for obtaining satisfactory bit error rate [18].) We believe that quite similar behavior will be observed in any other T&F distribution system exploiting an on/off intensity modulation, with only possibly a slightly different value of the threshold SNR.

Analyzing the presented plots, one may observe that for the 100-km interamplifier spans and basic SPBAs the total length of the link is limited to 300 km only. The main reason of this limitation is due to the noise generated by beating of the double-backscattered signals with the main signal. After adding WSIs (and thus blocking the doubly backscattered signals), the distance might be extended to 700 km. In case of shorter spans (80 km), the reachable distances are 400 and 1000 km, respectively. For even shorter spans (50 km), there is some additional improvement, but still the maximum distance is only slightly longer than 1000 km. This is because for short interamplifier spans and the double-backscattering eliminated by the WSIs, the dominant limiting factor is the PN-IN conversion, pronounced by high value of accumulated chromatic dispersion.

In a real installation, the lengths of the spans are of course not equal, but usually are in the range of 50–100 km. Thus, the general conclusion is that for distances exceeding 500 km a reliable operation of links equipped with SPBAs may become problematic. In addition, it may be noted that for badly conditioned links (long and/or substantially unequal spans, excess attenuations, or reflections), the gain of each amplifier must be carefully optimized before launching the operational connection [11], [12].

Our practical experience with setting up long-haul T&F links consists of six installations with the length in the range from 139 to 421 km. In these installations, we used both basic SPBAs, and in some critical locations the amplifiers were equipped with WSIs. The gains of the SPBAs and the locations of WSIs were deliberately optimized based on the prior knowledge of the span lengths and attenuation, by means of the prior-installation simulations. In all these cases, we managed to obtain the sufficient SNR, with at least a few decibel "safety margin." Thanks to that the links are operational for many years and survived many fiber repairs and other operator's actions without any intervention. The basic information about these installations is collected in Table I.

But we also faced with an extreme case (a link between London and Paris connecting English and French T&F facilities), where our simulations show very low SNR for standard SPBAs, and just-at-the-edge value of 19 dB in case of all the SPBAs equipped with WSIs (see the last row of Table I). For such an international link, with very difficult maintenance and limited access to the amplification points, such a low SNR is inacceptable from a practical perspective. This particular case triggered our investigations of additional solution, namely, the optical–electrical–optical (OEO) regeneration.

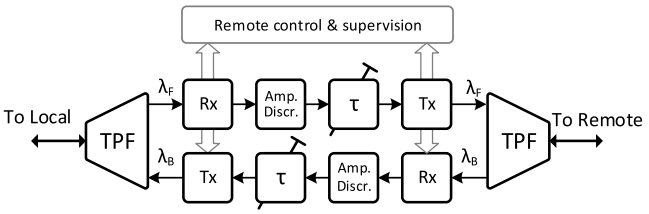

Fig. 4. Block diagram of the OEO regenerator. τ stands for small adjustable delays ($\pm$5 ps) used for equalizing the forward and backward propagation delays.

II. OEO REGENERATOR–IDEA AND ANALYSIS

The basic idea of the OEO regenerator is to convert the weak and noisy optical signal into the electrical domain, reshape it with a high-speed amplitude discriminator which strips-off the amplitude noise, and then to modulate the laser transmitter (Tx) to produce the full-power optical signal again. In our case, the regenerator should be bidirectional, and thus in fact the two basic blocks are combined with the TPFs (see Fig. 4).

The fundamental advantage of using the regenerator is illustrated in Fig. 5. In case of only optical amplification, the signal continuously accumulates the noise along the length of the optical path, as shown in the upper row. When the regenerator is introduced (lower row), the amplitude noise present at the OEO input is basically removed with the discriminator; however, because of amplitude-to-phase noise conversion some small residual phase noise is imprinted into the regenerated signal. Of course, to avoid false slopes and pulses at the output of the discriminator, the SNR at its input should be high enough, and thus the number and location of the OEO regenerators along the long link must be chosen in a way which guarantees that the SNR in each segment does not drop below the safe value, that is, below 17–18 dB mentioned above.

In comparing the OEO regenerators with SPBAs, two other advantages may be, in addition, pointed out. The first one is

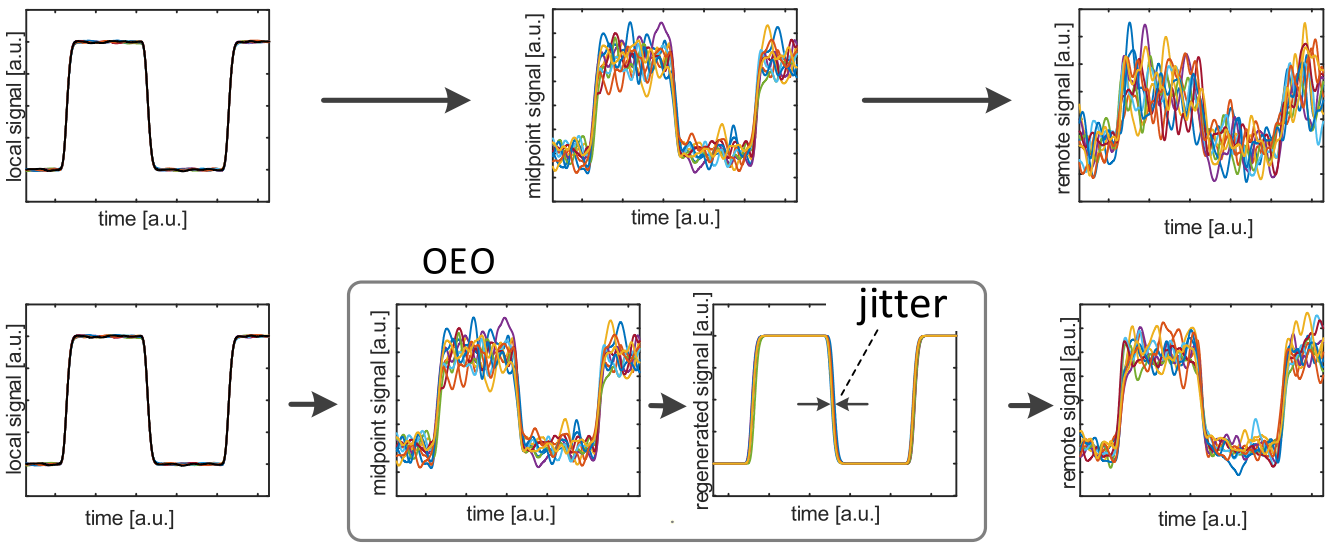

Fig. 5. Signal degradation along the optical path (left to right). Upper row without regenerator and lower row with the OEO regenerator.

that in a typical case of about −30 dBm sensitivity of the optical receiver and about 0-dBm transmitter output power, the equivalent gain of the regenerator is approximately 30 dB, which is more than ten times higher than the maximum gain of a bidirectional optical amplifier. The second one is related to the PN-IN conversion, due to the optical signal interaction with the chromatic dispersion. In case of a long fiber path, for instance 1000 km, the power spectral density (psd) of PN-IN is located in a relatively low-frequency range, up to approximately 1 GHz [15]–[17], and thus it falls into the bandwidth of the optical receiver. In case of shorter optical paths, the psd of PN-IN is spread in proportionally wider bandwidth, and thus only its small spectral part is passed by the limited-bandwidth receiver. (In our case, the receiver bandwidth is 1.5 GHz.) Consequently, breaking the long links with the OEO regenerators substantially reduces the impact of the PN-IN conversion.

The disadvantage of the bidirectional OEO regenerator is, however, that the paths for the forward and backward signals are not physically the same (see Fig. 4), so cannot be fully symmetrical, as it is in the SPBA. The impact of this asymmetry will be discussed and experimentally evaluated in Section III.

To illustrate the application of OEO regenerators, we once again simulate the links with 50- and 100-km-long spans. For shorter spans, the regenerator replaced the SPBA after 600 km, while for longer spans the regenerators were located after 300, 600, and 900 km. The resulting SNR is shown in Fig. 6(a), with green squares for 50-km-long spans and red circles for 100-km spans. Analyzing, for example, the situation with longer spans, one may notice that after 100, 200, and 300 km, the SNR is of course the same as in Fig. 3 (solid line with circles), but after passing the regenerator the SNR is restored. Then, after passing 400, 500, and 600 km, the SNR is again decreased, but is restored again in the next OEO regenerator, and so on. One may notice that this time the link length is, in principle, not limited by the SNR.

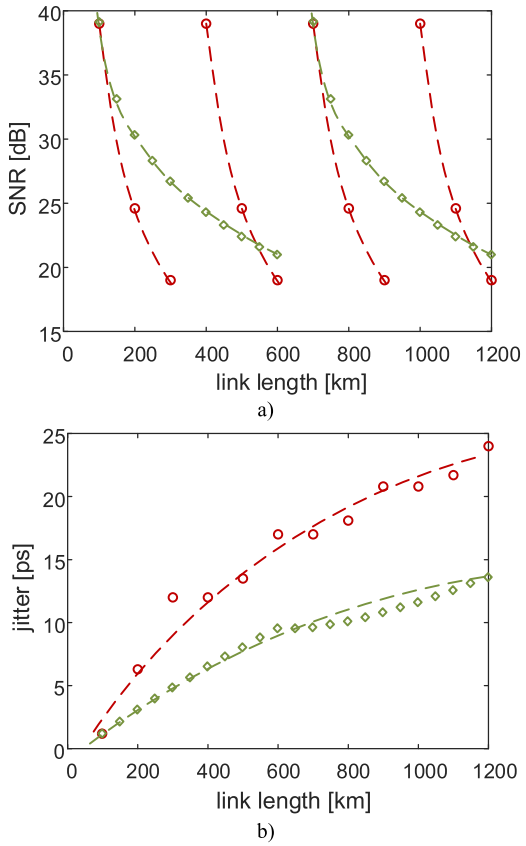

Fig. 6. (a) Simulated SNR and (b) output rms jitter for the links with OEO regenerators. Red circles are for 100-km-long spans and OEOs after each 300-km segment and green squares are for 50-km-long spans and one OEO after 600 km. One may notice that the increase in jitter is evidently mitigated after each regenerator, i.e., after 300, 600, and 900 km for red circles and after 600 km for green squares.

We also simulated the one-shot (i.e., not averaged) jitter at the receiver output for various link lengths [see Fig. 6(b)]. Analyzing again the situation with longer spans, it may be stated that for 100-, 200-, and 300-km-long links, the jitter results simply from intensity noise to phase noise conversion

at the receiver. But at the output of the regenerator placed after 300-km segment, this jitter becomes "imprinted" directly onto the slopes of the modulated optical signal (as illustrated in Fig. 5) and becomes statistically independent on the intensity noise being accumulated along the next segment. At the end of the second segment (i.e., after 600 km), this intensity noise is converted into the jitter in the second regenerator and adds statistically to the jitter inherited from the first segment. Thus, the jitter after two segments is $\sqrt{2}$ times higher than after the first one, and generally the jitter increases with the square root of the number of the segments.

Basically, similar observations may be done for the case with shorter spans, with the only difference that slower deterioration of the SNR allows using the OEO regenerators less frequently; in the case under consideration, only one regenerator is sufficient for the 1200-km-long link.

III. Experimental Results

To perform a practical verification of the presented ideas, we have built two OEO regenerating stations. We used transmitters with DFB telecom-grade lasers equipped with integrated electroabsorption modulators and thermo-electric coolers and 1.5-GHz bandwidth receivers with avalanche photodiodes. As the amplitude discriminators, we use high-speed limiting amplifiers (MAX3748, rated for up to 4 Gb/s data transmission), which allow the modulation of the lasers with constant amplitude and rise/fall times (60 ps), regardless of the input optical signal level. The signal chains of the regenerator are thus capable of carrying out frequency signals up to 1 GHz, or equivalently data sequences with up to 2 Gb/s rate. The lasers' wavelengths are stabilized at two neighbor dense wavelength division multiplexing (DWDM) channels (100-GHz separation), and the standard three-port thin-film filters widely used as DWDM add-drop multiplexers were applied. All the parts were enclosed in a metal 19-in 2U case, to ensure equal temperature conditions for forward and backward signal paths.

An important requirement, needed for accurate time transfer is calibration, that is, precise determining of the delay of the output timetags with respect to a reference UTC(k) timescale. Such calibration is based on the measuring of a round-trip delay of the time signal, dividing the obtained value by two, and applying corrections related to the identified asymmetries between the forward and backward signal paths. From this point of view, the best option is to assure exactly equal forward and backward delays in the regenerator and thus get rid of the additional corrections. A careful matching of all the electrical and optical connections within the regenerator allows obtaining a residual mismatch of below 10 ps, and this can further be reduced by placing the small variable capacitors in both the signal paths acting as adjustable delays (see Fig. 4). As a direct measurement of the propagation delays of the regenerator is cumbersome, we placed the regenerator (with additional attenuators) in the middle of the optical path over which the ELSTAB system was operated and trimmed the capacitors until we obtained the situation that placing the regenerator did not affect the calibration. We assessed the accuracy of the forward–backward delay matching obtained this way to about 2 ps.

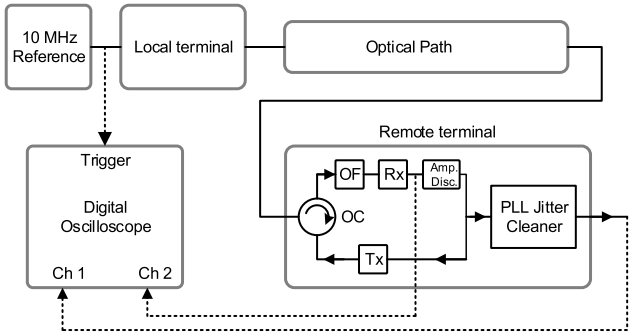

Fig. 7. Simplified schematic of the measurement setup. Signal path related to 1 PPS ignored for clarity.

In the first experiment, we performed the measurements analogous to the simulations shown in Fig. 6(a) and (b). We connected the ELSTAB terminals (the local and the remote ones) with the optical path containing 100-km-long spooled fiber sections, with the SPBAs and regenerators in between. The fibers used were both standard ones (G.652; 10 × 50 km) and also dispersion-shifted (G.655; 8 × 50 km). The two regenerators were placed between 300-km segments, and the total fiber length was 900 km. The gains of the SPBAs were optimized for the best SNR and were in the range of 17–18.5 dB. In the first step, the remote terminal was placed after 100 km of the fiber, and then the length of the link was extended gradually, with the SPBAs and OEOs placed accordingly to the scheme taken during the simulations described in Section II. We measured the SNR and jitter at the output of the optical receiver (avalanche photodiode plus transimpedence amplifier) in the ELSTAB remote terminal. In addition, we measured the final jitter at the user's output of the remote terminal, which is internally processed by the phase-locked loop (PLL) acting as a jitter cleaner. The jitter was measured with a DSOS404A oscilloscope, with respect to the 10-MHz reference signal, provided both to the local module and to the oscilloscope's trigger. The noise floor of the jitter measurement setup was about 1.8 ps. Its schematic is presented in Fig. 7.

The measurement results are shown in Fig. 8 and are generally consistent with the simulations presented in Fig. 6. The SNR improvement after each regenerator is clearly visible. The SNR is not exactly equal after each 300-km segment, which is related to not equal output powers of the laser transmitters used and also slightly higher attenuation of the segments with greater number of G.655 spools. The measured values of the receiver output jitter are only slightly higher than the simulated and generally grow proportionally to the square root of the total length. The jitter at the user's output of the remote terminal, thanks to the jitter cleaner, is approximately three times smaller than the jitter measured directly at the receiver output, and even for the 900-km-long link is well below 10 ps.

We also performed long-term observations oriented on possible detection of missed 1 PPS pulses or discontinuity (phase jumps) of the 10-MHz output frequency and found no evidence of such events in a 10-h-long observation period. However, in case of even small additional attenuation (in the order of 3 dB) placed anywhere along the optical path, such

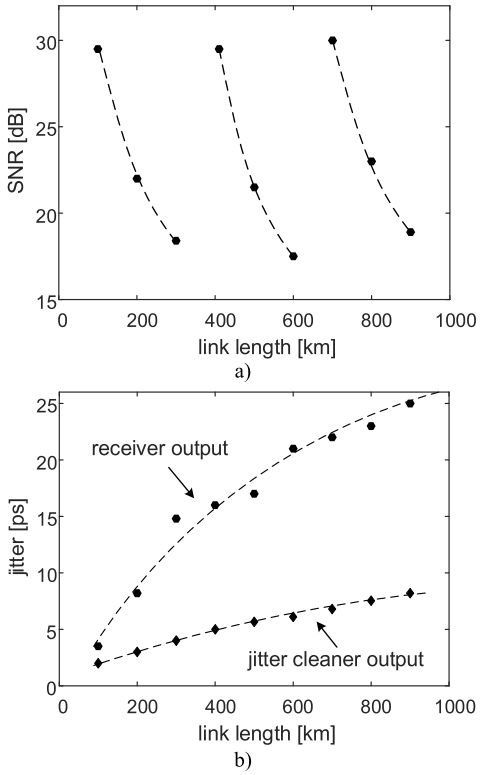

Fig. 8. (a) SNR and (b) rms jitter measured along the 900-km-long link.

events were sporadically visible and could not be eliminated by increasing the gains of the SPBAs. This is due to the fact that 3 × 100-km segments taken in this experiment place the system just at the edge of the acceptable SNR, and thus there is no room for any further detrimental factors. (One can deduct from Fig. 8(a), however, that placing OEOs after each 200-km segment would improve the SNR substantially and make a room for some additional attenuations along the link.)

In the next step, we examined the stability of the forward–backward propagation symmetry of the regenerator. Basically, the impact of temperature should be the same for both the directions and should not affect the symmetry, but second-order effects might build up a small residual thermal asymmetry. As the regenerators are intended to be located in telecom shelters with poor thermal conditions, this issue is of high practical importance. In the experiment, we placed the ELSTAB terminals and the fiber spools in a temperature-stable laboratory and the regenerator in a thermal chamber where the temperature changed by 5 K with a saw-tooth profile and the full-cycle period of 4 h. We observed the fluctuations of the phase of 10-MHz signal at the output of the remote terminal. The measurement lasted two days, and we calculated the time deviation (TDEV) to clearly separate the fluctuations correlated with 4-h periods. The results are shown in Fig. 9, where the bump related to the chamber operation can be identified. Based on these results, the impact of the regenerator's temperature may be estimated as 30 fs/K. We repeated this experiment for various levels of the optical power received from the forward and backward directions, obtaining still similar results. Concluding, one may notice that the impact of the regenerator temperature on the transfer

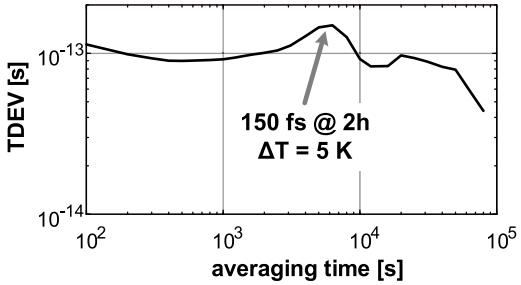

Fig. 9. TDEV measured with OEO undergoing 5-K temperature cycles with 4-h period.

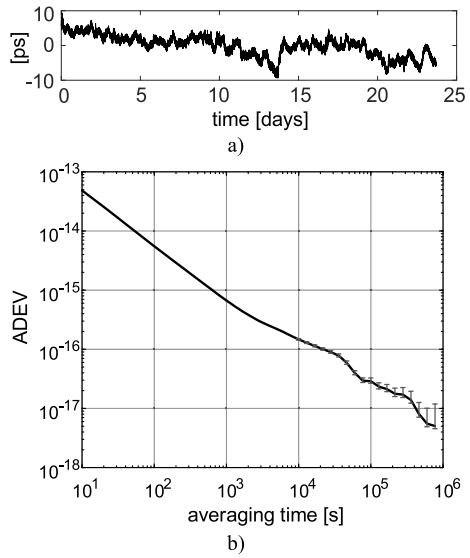

Fig. 10. (a) Time-domain phase fluctuations and (b) ADEV of 10-MHz output frequency measured for 520-km-long link with four optical amplifiers and one OEO regenerator.

stability is noticeable, but even for 5-K temperature variations it is small and does not stand out from the other factors affecting the overall stability.

In the final experiment, we cascaded two sections of 100-km spooled fibers, 60 km of fiber being a part of a real urban network around Krakow, again two sections of 100-km spooled fibers, and again 60 km of the urban fiber (the total length 520 km). The sections of the urban fiber were patched at many places and thus have the attenuation of 18 dB, which is closed to the attenuation of 100 km of spooled fiber (being around 20 dB). In the first step, we placed five SPBAs between the sections. In this case, we were not able to make the link operational, as the SNR was insufficient regardless of the amplifiers' gains. This observation is in full agreement with our simulations.

In the next step, we replaced the amplifier located in the middle of the optical path with the OEO regenerator. This time the link operated correctly, and we registered the stability of the phase of the remote output signal with respect to the input 10-MHz signal for 24 days. The spools, optical amplifiers, and the regenerator were placed in nonair-conditioned rooms (temperature fluctuations of about 5 K), whereas the ELSTAB terminals and the oscilloscope registering the phase fluctuations were located in the laboratory with a stable temperature (temperature fluctuations below 0.5 K). The phase

registered during this part of the experiment, together with calculated overlapping Allan deviation (ADEV), is shown in Fig. 10(a) and (b), respectively.

The stability is similar as in our previous long-haul experiments without an OEO regenerator (see [5], and [19]), so one may conclude that the impact of the regenerator on the transfer stability is insignificant. The one-day stability is 3×10^{-17}, and a subtle bump at the half-a-day averaging is noticeable. As the thermal sensitivity of the regenerator was evaluated earlier and occurred to be extremely small, the reason of this instability is related rather to the imperfect compensation of the large delay fluctuations, occurring in the spools exposed to daily temperature fluctuations in the nonstabilized room.

Commenting on the generality of the presented experimental results, one may note that the proposed OEO regenerator, although tested within the ELSTAB-based setup, is itself not directly related to the ELSTAB technology. It consists of standard opto-electronic components, commonly used in fiber-optic data transmission, and may be used for transmitting any square wave signal or data sequences up to 1 GHz or 2 Gb/s, with the same evolution of SNR and jitter along the link.

IV. Conclusion

In this article, we discussed the limitations of bidirectional optical amplification usually used in the long-haul fiber-optic links distributing metrological T&F signals by means of intensity modulation. Using our simulation tools developed previously, we demonstrated that the maximum length of the link with optical amplifiers would be approximately 300–1000 km, depending on the span lengths and design of the amplifier (i.e., without or with WSI). Especially, the maximum reach of the links with long spans between amplification points (in the order of 100 km) would be seriously limited. Unfortunately, the newest telecom fiber networks tailored for coherent DWDM systems have severely limited density of regeneration points, which make this problem even more pronounced.

In this context, we presented a combined regeneration solution, where some of the optical amplifiers were replaced with OEO regenerators. This allowed to sustain the required SNR basically along an unlimited distance. In this situation, the increasing length of the link results in the build-up of jitter on the remote metrological signal, but the jitter grows with a square root of the distance, and thus is reasonably small even for long links, especially if a jitter-cleaning PLL is used.

Two OEO regenerators were built and extensive experimental verification of the expected performance of the combined regeneration was performed with the ELSTAB terminals at the ends of the link. We demonstrated the restoration of the SNR obtained with the OEO regenerators and observed the jitter performance as predicted. In addition, we tested the thermal sensitivity of the OEO regenerator and found hardly noticeable impact on the frequency signal stability (TDEV), namely, 150 fs for 5-K temperature cycles.

Some practical issue related to the ELSTAB technology is that in course of calibration of time transfer, we perform the automatic measurement of the chromatic dispersion of the actual optical path. For this purpose, the wavelength of the local terminal laser is temporary shifted. In case of the link with OEO regenerators also the forward-direction lasers in the regenerators must be shifted as well. There are no technical problems related to our devices, but the remote control of the regenerator must be guaranteed at least for the period of the calibration procedure, which needs to be run after initial installation or a significant change in the optical path.

Our analysis and experiments were related to the ELSTAB technology, but the outcomes are fully applicable to any other T&F distribution systems based on the on/off intensity modulation of the optical signals, for example, IEEE 1588 White Rabbit technology [20].

References

[1] M. Fujieda, M. Kumagai, T. Gotoh, and M. Hosokawa, "Ultrastable frequency dissemination via optical fiber at NICT," *IEEE Trans. Instrum. Meas.*, vol. 58, no. 4, pp. 1223–1228, Apr. 2009.

[2] S. M. F. Raupach and G. Grosche, "Chirped frequency transfer: A tool for synchronization and time transfer," *IEEE Trans. Ultrason., Ferroelectr., Freq. Control*, vol. 61, no. 6, pp. 920–929, Jun. 2014.

[3] O. Lopez *et al.*, "Frequency and time transfer for metrology and beyond using telecommunication network fibres," *Comp. Rendus Phys.*, vol. 16, no. 5, pp. 531–539, Jun. 2015.

[4] X. Chen *et al.*, "Simultaneously precise frequency transfer and time synchronization using feed-forward compensation technique via 120 km fiber link," *Sci. Rep.*, vol. 5, no. 1, Nov. 2016, Art. no. 18343.

[5] P. Krehlik, L. Sliwczynski, L. Buczek, J. Kolodziej, and M. Lipinski, "ELSTAB—Fiber-Optic time and frequency distribution technology: A general characterization and fundamental limits," *IEEE Trans. Ultrason., Ferroelectr., Freq. Control*, vol. 63, no. 7, pp. 993–1004, Jul. 2016.

[6] J. Kodet, P. Pánek, and I. Procházka, "Two-way time transfer via optical fiber providing subpicosecond precision and high temperature stability," *Metrologia*, vol. 53, no. 1, pp. 18–26, Feb. 2016.

[7] S. W. Schediwy, D. R. Gozzard, S. Stobie, J. A. Malan, and K. Grainge, "Stabilized microwave-frequency transfer using optical phase sensing and actuation," *Opt. Lett.*, vol. 42, no. 9, pp. 1648–1651, 2017.

[8] M. Lessing, H. S. Margolis, C. T. A. Brown, and G. Marra, "Frequency comb-based time transfer over a 159 km long installed fiber network," *Appl. Phys. Lett.*, vol. 110, no. 22, May 2017, Art. no. 221101.

[9] P. Krehlik, Ł. Śliwczyński, Ł. Buczek, and J. Kołodziej, "Fiber-optic UTC(k) timescale distribution with automated link delay cancelation," *IEEE Trans. Ultrason., Ferroelectr., Freq. Control*, vol. 66, no. 1, pp. 163–169, Jan. 2019.

[10] K. Predehl *et al.*, "A 920-kilometer optical fiber link for frequency metrology at the 19th decimal place," *Science*, vol. 336, no. 6080, pp. 441–444, Apr. 2012.

[11] Ł. Śliwczyński and J. Kołodziej, "Bidirectional optical amplification in long-distance two-way fiber-optic time and frequency transfer systems," *IEEE Trans. Instrum. Meas.*, vol. 62, no. 1, pp. 253–262, Jan. 2013.

[12] Ł. Śliwczyński, P. Krehlik, and K. Salwik, "Modeling and optimization of bidirectional fiber-optic links for time and frequency transfer," *IEEE Trans. Ultrason., Ferroelectr., Freq. Control*, vol. 66, no. 3, pp. 632–642, Mar. 2019.

[13] M. Amemiya, M. Imae, Y. Fujii, T. Suzuyama, F. Hong, and M. Takamoto, "Precise frequency comparison system using bidirectional optical amplifiers," *IEEE Trans. Instr. Meas.*, vol. 59, no. 3, pp. 632–640, Mar. 2010.

[14] X. Ding, G.-L. Wu, F.-X. Zuo, and J.-P. Chen, "Bidirectional optical amplifier for time transfer using bidirectional WDM transmission," *Optoelectron. Lett.*, vol. 15, no. 6, pp. 401–405, Nov. 2019.

[15] S. Yamamoto, N. Edagawa, H. Taga, Y. Yoshida, and H. Wakabayashi, "Analysis of laser phase noise to intensity noise conversion by chromatic dispersion in intensity modulation and direct detection optical-fiber transmission," *J. Lightw. Technol.*, vol. 8, no. 11, pp. 1716–1722, Jun. 1990.

[16] W. K. Marshall, B. Crosignani, and A. Yariv, "Laser phase noise to intensity noise conversion by lowest-order group-velocity dispersion in optical fiber: Exact theory," *Opt. Lett.*, vol. 25, no. 3, pp. 165–167, 2000.

[17] P. Krehlik and Ł. Śliwczyński, "Precise method of estimation of semiconductor laser phase-noise-to-intensity-noise conversion in dispersive fiber," *Measurement*, vol. 65, pp. 54–60, Apr. 2015.

[18] G. P. Agrawal, *Fiber-Optic Communication Systems*, 4th ed. Hoboken, NJ, USA: Wiley, 2010.

[19] P. Krehlik, Ł. Śliwczyński, Ł. Buczek, J. Kołodziej, and M. Lipiński, "Ultrastable long-distance fibre-optic time transfer: Active compensation over a wide range of delays," *Metrologia*, vol. 52, no. 1, pp. 82–88, Feb. 2015.
[20] E. F. Dierikx *et al.*, "White rabbit precision time protocol on long-distance fiber links," *IEEE Trans. Ultrason., Ferroelectr., Freq. Control*, vol. 63, no. 7, pp. 945–952, Jul. 2016.

Przemysław Krehlik received the M.Sc. and Ph.D. degrees in electronics from the AGH University of Science and Technology, Kraków, Poland, in 1988 and 1998, respectively.

Since 1988, he has been with Fiber Optic Transmission Group, Department of Electronics, AGH University of Science and Technology. He has authored or coauthored more than 70 papers in journals and conference proceedings. His research interests include electronic circuits, direct modulation of semiconductor lasers, and application specific fiber-optic systems.

Łukasz Śliwczyński (Member, IEEE) received the M.Sc. and Ph.D. degrees from the AGH University of Science and Technology, Kraków, Poland, in 1993 and 2001, respectively.

He was working on various high-speed transmitters and receivers for digital fiber-optic transmission systems. Since about ten years, he has been working on precise time and frequency transfer systems exploiting optical fibers. He has authored or coauthored more than 70 papers in journals and conference proceedings.

Łukasz Buczek was born in Kraków, Poland, in 1984. He received the M.Sc. and Ph.D. degrees from the AGH University of Science and Technology, Kraków, in 2009 and 2018, respectively.

In 2009, he joined Fiber Optic Transmission Group, AGH University of Science and Technology. His research interest includes precise stabilization of wavelength of semiconductor laser sources.